IEEE Access
Multidisciplinary | Rapid Review | Open Access Journal

Received September 14, 2021, accepted October 10, 2021, date of publication October 15, 2021, date of current version October 22, 2021.

Digital Object Identifier 10.1109/ACCESS.2021.3120366

Analysis and Calibration of Blade Tip-Timing Vibration Measurement Under Variable Rotating Speeds

ZHONGSHENG CHEN, (Member, IEEE), YEMEI XIA, HAO SHENG, AND JING HE

College of Electrical and Information Engineering, Hunan University of Technology, Zhuzhou 417002, China

Corresponding authors: Zhongsheng Chen (chenzswind@gmail.com) and Jing He (hejing@263.net)

This work was supported by the National Natural Science Foundation of China under Grant 51975206.

ABSTRACT Blade tip timing (BTT) vibration measurement is a promising on-line blade monitoring method, but various uncertainties bring great challenge in engineering applications. Most existing works are based on the assumption of constant rotating speeds. However, rotating speed is hardly fixed under variable conditions. In this case, these uncertainties always become more serious. To deal with this problem, this paper proposes to investigate BTT measurement derivations in angular domain, instead of time domain. Firstly, this paper systematically analyzes the effects of variable rotating speed, static angle errors and translational blade motions on the accuracy of BTT vibration measurement. Then the corresponding calibration methods are presented by only using times of arrival (TOAs). In the end, Matlab/Simulink simulations are done to validate the proposed method under linear and quadratic variations of rotating speeds. The results demonstrate that BTT measurement deviation under low rotating speeds is more than those under high rotating speeds and BTT measurement deviation due to static angle errors is independent of rotating speeds. And the proposed TOAs-based calibration method can reduce BTT measurement deviation greatly under variable rotating speeds, compared with traditional methods. BTT measurement deviation due to static angle errors can be calibrated by using low rotating speeds and those due to translational blade motions are difficult to be calibrated under variable rotating speeds. Thus simulation results indicate great potential of the proposed method for practical applications of the BTT method.

INDEX TERMS Blade tip-timing, variable rotating speed, measurement uncertainty, angular sampling, vibration calibration.

I. INTRODUCTION

Blades are one class of key mechanical components in aero-engines, including fan, compressor and turbine blades. According to working modes, they can be divided into stationary and rotating blades. During day-to-day operation, rotating blades often interact with the air flow continuously. Then uneven and unstable air flow distribution and unbalanced centrifugal force of the rotor always make each blade vibrate, resulting in high-cycle fatigues. In addition, during take-off, landing or low altitude flight, small hard particles are often inhaled by the engines, which may cause foreign object damage (FOD) of fan/compressor blades. Fatigue and FOD make blades become one of the most easily-worn parts in aero-engine structures. Statistical data show that faults caused by vibration account for more than 60% of the total aero-engine faults. Moreover, more than 70% of blade faults are induced by vibrations [1], [2]. Blade damage or failure is very dangerous to flight safety and a broken blade may damage all blades, even breaking through the whole engine. Therefore, on-line blade vibration monitoring is very significant for safety, reliability, and availability [3]. But how to realize it under high-speed rotation is always a big challenge.

Blade tip timing (BTT) vibration measurement is a promising non-contact and on-line monitoring method [4]–[8]. Its basic principle is to install a timing reference sensor and several BTT probes, and then measure times of arrival (TOAs) of each blade passing each BTT probe. When blade vibration happens, the blades will pass BTT probes earlier or later than theoretical times. In this case, a TOA difference series will be generated for each blade. Based on it, blade vibration displacements can be calculated. Therefore, the BTT method

The associate editor coordinating the review of this manuscript and approving it for publication was Yue Zhang.

has the advantages of easy installation, low measurement cost, monitoring all rotating blades simultaneously. Up to now, the BTT method has been widely studied in research and industrial communities. Chen *et al.* gave a comprehensive review on blade tip timing-based health monitoring [5].

According to basic principle, accurate TOAs of a blade is the primary prerequisite for BTT vibration measurement. In practice, however, theoretical and actual TOAs are definitely affected by many factors, which has been discussed in [5]. For example, there may be installation angle errors of BTT and timing reference probes due to manufacturing and installation errors. In this case, theoretical TOAs are often inaccurate. As for actual TOAs, BTT sensing positions may change during rotation due to complex aerodynamic excitations [9], [10], which also affect actual TOAs. Therefore, it is much necessary to analyze negative effects of key factors on BTT vibration measurement. In recent years, more and more attention has being paid on BTT measurement uncertainties [11], [12]. By now, several related studies have been reported. Russhard evaluated qualitatively several uncertainties, including probe type, probe position, waveform quality, acquisition and data processing [11]. Zhou *et al.* analyzed theoretically the BTT uncertainty from rotational speed fluctuation and carried out Simulink-based simulations [13]. Mohamed *et al.* pointed out the equilibrium position shift of the blade tip resulted in vibration measurement errors. But they only focused on determining simultaneous steady-state movements using BTT data [9], [10]. Pickering developed innovative test methods to experimentally evaluate the performance of the BTT method due to blade and probe static offsets [14]. It should be noted that most existing works were based on the assumption of constant rotating speeds. Mohamed *et al.* pointed out that high-rate speed change was more problematic in BTT measurement due to the variation of the associated positional error with rotating speed [15]. To deal with BTT signals under variable speeds, Chen *et al.* have proposed to perform angular-domain analysis, instead of time-domain analysis [16]–[18]. Fan *et al.* applied a polynomial fitting using once-per-revolution (OPR) sensor's data to approximate the speed change in one revolution [19]. Zhang *et al.* used multiple reference phases for online BTT monitoring under variable-speed operation [20]. To our best knowledge, few systematic studies were done on the influence mechanism of variable speeds, especially the corresponding calibration methods.

In the previous work [18], the authors have mentioned the effects of variable rotating speeds on angular-domain BTT vibration measurement. However, it was preliminary and incomplete. The innovation of this paper is to advance the above work to systematically analyze the effects of rotating speed, static angle errors and translational blade motions on BTT vibration measurement under variable rotating speeds. Furthermore, the corresponding calibration methods are presented, respectively. The paper is structured as follows. Section II summarizes key influencing factors of BTT vibration measurement and outlines research gap of existing methods. Section III carries out derivation analysis of BTT vibration measurement under variable rotating speeds. Section IV presents the corresponding calibration methods for variable rotating speeds, static angles and translational blade motions. Matlab/Simulink simulations are done to validate the proposed method in Section V. Finally, brief conclusions are presented in Section VI.

II. RESEARCH GAP

Basic structure of fiber-optic-based BTT vibration measurement is shown in Figure 1 [18], which is mainly composed of multiple fiber-optic BTT probes, a timing reference sensor (also known as the OPR sensor), a signal receiving and conversion module, and an analysis software. Fiber-optic BTT probes are used to measure TOAs of each blade and the OPR sensor is used to provide the time reference. Generally speaking, there is at least a OPR mark on the rotating shaft. When the OPR sensor passes the mark, a timing pulse is generated as the time reference. Assuming that the speed is constant, theoretical TOAs of each blade are fixed when the blade does not vibrate. While the blade vibrates, there are time differences between actual and theoretical TOAs. Furthermore, these time differences are strongly related to vibration frequency and amplitude of the blade, so that they can be used to calculate blade vibration displacements. It should be noted that accurate TOAs are very important. In this paper, measurement errors of TOAs due to noises are assumed to be negligible.

For the sake of easy understanding, let the blisk rotate clockwise at a constant rotating frequency (f_n) in the nth revolution. When no vibrations, theoretical TOAs of the kth blade passing the ith BTT probe can be calculated as

$$t_{i,k,n}^{the} = \begin{cases} \sum_{p=1}^{n-1} \frac{1}{f_p} + \frac{\alpha_i - \theta_k}{2\pi f_n}, & \theta_k \le \alpha_i \\ \sum_{p=1}^{n} \frac{1}{f_p} + \frac{\alpha_i - \theta_k}{2\pi f_n}, & \theta_k > \alpha_i \end{cases} \tag{1}$$

where f_p denotes the rotating frequency of the pth revolution. α_i and θ_k are angles of the ith BTT probe and the kth blade relative to the OPR mark, respectively.

The corresponding actual TOAs are denoted as $t_{i,k,n}^{act}$, and then vibration displacement of the kth blade measured by the ith BTT probe can be calculated as,

$$d_{i,k}[n] = 2\pi f_n R(t_{i,k,n}^{act} - t_{i,k,n}^{the}) \tag{2}$$

where R is the rotating radius of the blade tip.

Based on Equation (1) and Equation (2), we can see BTT measurement uncertainties mainly come from α_i, θ_k and R if f_n is a constant. At the same time, uncertainties due to α_i and θ_k often come from installment errors of BTT or OPR probe and uncertainties due to R come from blade motions. Russhard pointed out that it was possible to reduce and control these uncertainties [11].

In practice, f_n is indeed not constant due to variable conditions. In this case, measurement uncertainties also come

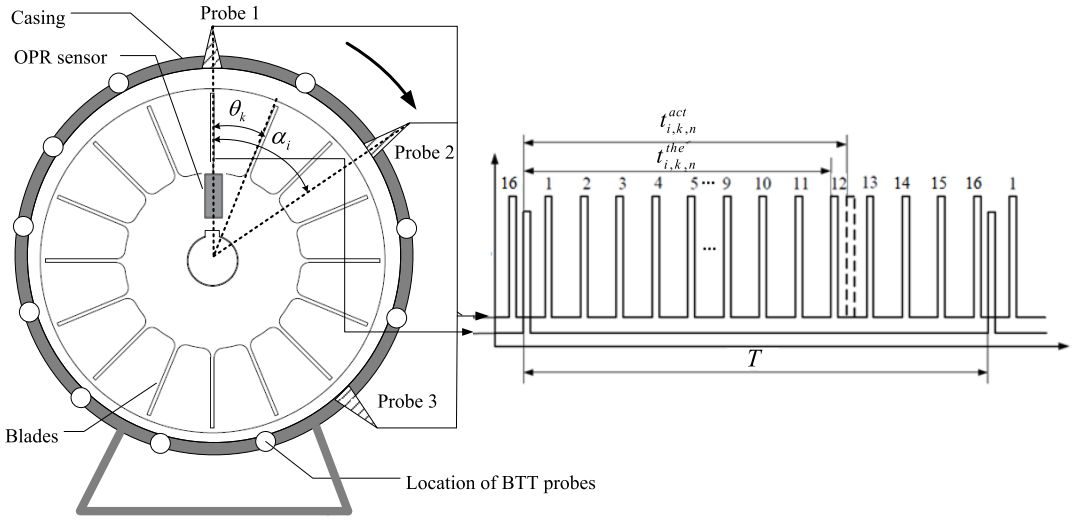

FIGURE 1. Basic structure of the BTT method [18].

from f_n according to Equation (1) and Equation (2). As stated by Mohamed *et al.* [15], variable rotating speeds greatly complicated BTT measurement uncertainty analysis. Existing methods cannot solve this issue well. Thus this paper just aims to deal with it.

As shown in Figure 1, BTT probes are mounted around the circumference of the bladed disk, so BTT sampling can be looked as a natural angular-sampling process. Thus this paper adopts angular-domain method presented in the previous work [18]. Then similar to TOAs, theoretical angles of arrival (AOAs) of the kth blade passing the ith BTT probe under no vibrations can be represented as,

$$\theta^{the}_{i,k,n} = \begin{cases} 2\pi\ (n-1) + \alpha_i - \theta_k, (n = 1, 2, \ldots), & \theta_k \le \alpha_i \\ 2\pi n + \alpha_i - \theta_k, (n = 1, 2, \ldots), & \theta_k > \alpha_i \end{cases} \tag{3}$$

In order to illustrate the principle clearly, the angular speed is denoted as $\omega\,(t)$. Then actual AOAs of the kth blade passing the ith BTT probe can be calculated as,

$$\theta^{act}_{i,k,n} = 2\pi\ (n-1) + \int_{t_{n-1}}^{t_{n-1}+\Delta t^{ik}_n} \omega\,(t)\,dt \tag{4}$$

where t_{n-1} is the measured ending time of the (n-1)th revolution, Δt^{ik}_n is the net time of the kth blade arriving at the ith BTT probe in the nth revolution.

By combining Equation (3) and Equation (4), vibration displacement of the kth blade measured by the ith BTT probe can be calculated as,

$$\begin{aligned} \tilde{d}_{i,k}\,[n] &= \left(\theta^{act}_{i,k,n} - \theta^{the}_{i,k,n}\right) \times R \\ &= \begin{cases} \left(\int_{t_{n-1}}^{t_{n-1}+\Delta t^{ik}_n} \omega\,(t)\,dt - (\alpha_i - \theta_k)\right) R, & \theta_k \le \alpha_i \\ \left(\int_{t_{n-1}}^{t_{n-1}+\Delta t^{ik}_n} \omega\,(t)\,dt - (2\pi + \alpha_i - \theta_k)\right) R, & \theta_k > \alpha_i \end{cases} \end{aligned} \tag{5}$$

According to Equations (3)∼(5), we can see BTT vibration measurement in angular domain are closely related to the rotating speed, the positions of BTT probes and OPR sensor, and the rotating tip radius. In particular, the most advantage of angular-domain method is that $\theta^{the}_{i,k,n}$ is independent of $\omega\,(t)$ in Equation (3). In this case, the difficulty due to variable rotating speeds can be decreased. Next, we will study these influence factors and calibrate the corresponding deviations in order to improve the accuracy of BTT vibration measurement. Compared with existing works, unique features of this study mainly include: i) investigating BTT measurement uncertainties in angular domain as for variable rotating speeds, instead of time domain; ii) revealing the effects of two classes of variable rotating speeds on BTT measurement; iii) proposing calibration methods for rotating speeds and static angle errors under variable rotating speeds, respectively.

III. DERIVATION ANALYSIS OF BTT VIBRATION MEASUREMENT

A. EFFECTS OF VARIABLE ROTATING SPEED

According to Equation (3), theoretical AOAs are only related to static position angles of BTT probes and OPR sensor. Actual AOAs can be calculated as Equation (4) by using measured TOAs. In practice, angular speed of the nth revolution is often calculated as $\bar{\omega}_n = 2\pi/(t_n - t_{n-1})$ when using a single OPR sensor. Then actual AOAs are approximated as follows based on Equation (4).

$$\theta^{act}_{i,k,n} = 2\pi\ (n-1) + \bar{\omega}_n \Delta t^{ik}_n \tag{6}$$

Comparing Equation (6) with Equation (4), we can see that there are approximation derivations due to calculated actual AOAs, which is defined as,

$$\Delta\tilde{d}_{i,k}\,[n] = \left(\int_{t_{n-1}}^{t_{n-1}+\Delta t^{ik}_n} \omega\,(t)\,dt - \bar{\omega}_n \Delta t^{ik}_n\right) R \tag{7}$$

Moreover, the approximation derivations depend on the variation degree of the rotating speed. Furthermore, two classes of variable rotating speeds are considered, namely linear variation and quadratic variation as shown in Figure 2.

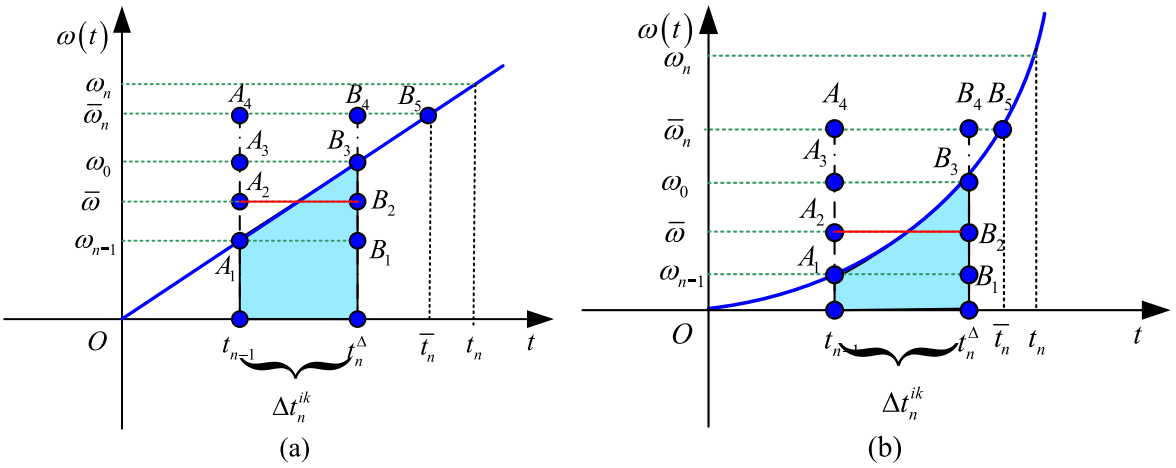

FIGURE 2. Two classes of variable rotating speeds: (a) linear variation and; (b) quadratic variation.

Here $\omega_{n-1}, \omega_0, \omega_n$ are instantaneous angular speeds at the times of $t_{n-1}, t_n^{\Delta}, t_n$, respectively. $\bar{\omega}$ is the average angular speed and $\bar{\omega} = (\omega_{n-1} + \omega_0)/2$. $A_1 \sim A_4$ and $B_1 \sim B_5$ denote the marking flags. It can be seen from Figure 2 that: 1) The real angle calculated by $\int_{t_{n-1}}^{t_n^{\Delta}} \omega(t)\, dt$ is equal to the enclosed area by $\{A_1, t_{n-1}, t_n^{\Delta}, B_3\}$, while the angle calculated by $\bar{\omega}_n \Delta t_n^{ik}$ is equal to the enclosed area by $\{A_4, t_{n-1}, t_n^{\Delta}, B_4\}$. Obviously, the latter is more than the former, so measurement derivation is definitely introduced into angular-domain vibration displacements. 2) The derivation under quadratic variation is more than that under linear variation. In summary, the faster the rotating speed changes, the more the measurement derivation are. In this case, the effects of variable rotating speed on BTT vibration measurement cannot be ignored.

B. EFFECTS OF STATIC POSITION ANGLES

According to Equation (5), static position angles leading to measurement deviation include the angle (α_i) of the ith BTT probe relative to the OPR sensor and the angle (θ_k) of the kth blade relative to the OPR mark.

Firstly, angular derivation of the ith BTT probe is denoted as $\Delta\alpha_i$. Under variable rotating speeds, theoretical AOAs of the kth blade passing the ith BTT probe in the nth revolution can be written as,

$$\bar{\theta}_{i,k,n}^{the} = \begin{cases} 2\pi\,(n-1) + \alpha_i + \Delta\alpha_i - \theta_k, (n = 1, 2, \ldots), \beta_k \le \alpha_i \\ 2\pi n + \alpha_i + \Delta\alpha_i - \theta_k, (n = 1, 2, \ldots), \beta_k > \alpha_i \end{cases} \tag{8}$$

Then vibration displacement of the kth blade measured by the ith BTT probe can be calculated as,

$$\begin{aligned} \bar{d}_{i,k}[n] &= \left(\theta_{i,k,n}^{act} - \bar{\theta}_{i,k,n}^{the}\right) \times R \\ &= \begin{cases} \left(\int_{t_{n-1}}^{t_{n-1}+\Delta t_n^{ik}} \omega_n(t)\, dt - (\alpha_i + \Delta\alpha_i - \theta_k)\right) R, \beta_k \le \alpha_i \\ \left(\int_{t_{n-1}}^{t_{n-1}+\Delta t_n^{ik}} \omega_n(t)\, dt - (2\pi + \alpha_i + \Delta\alpha_i - \theta_k)\right) R, \\ \qquad (n = 1, 2, \ldots), \beta_k > \alpha_i \end{cases} \end{aligned} \tag{9}$$

Based on Equation (5) and Equation (9), BTT vibration measurement deviation can be calculated as,

$$\left|\bar{d}_{i,k}[n] - d_{i,k}[n]\right| = \Delta\alpha_i R \tag{10}$$

It can be seen from Equation (10) that measurement deviation due to $\Delta\alpha_i$ is independent of variable rotating speed. When the tip radius (R) is fixed, the measurement deviation should be a constant.

Next, angular derivation of the kth blade is denoted as $\Delta\theta_k$. Under variable rotating speeds, theoretical AOAs of the kth blade passing the ith BTT probe in the nth revolution can be written as,

$$\tilde{\theta}_{i,k,n}^{the} = \begin{cases} 2\pi\,(n-1) + \alpha_i - \theta_k - \Delta\theta_k, (n = 1, 2, \ldots), \beta_k \le \alpha_i \\ 2\pi\,(n-1) + 2\pi + \alpha_i - \theta_k - \Delta\theta_k, (n = 1, 2, \ldots), \\ \qquad \beta_k > \alpha_i \end{cases} \tag{11}$$

Similarly, vibration measurement deviation can be calculated as,

$$\left|\tilde{d}_{i,k}[n] - d_{i,k}[n]\right| = \Delta\theta_k R \tag{12}$$

We can see that vibration measurement deviation due to $\Delta\theta_k$ is also independent of variable rotating speeds.

C. EFFECTS OF TRANSLATIONAL BLADE MOTIONS

As for fiber-optic BTT probes, laser light is emitted from the central fiber. The light beam will fall on the blade tip and the corresponding reflected light travels back to a photodiode through the outer fibers. Then a signal preprocessing circuit is utilized to analyze these reflected light signals and generate pulses. TOAs of each blade are obtained by these timing pulses. Theoretically, the light spot position on each blade tip should remain unchanged during rotation, namely the BTT sensing position. In practical applications, however, the blade may produce translational movements due to complex loads. In this case, the BTT sensing position will change, leading to deviations of actual TOAs which significantly affect the

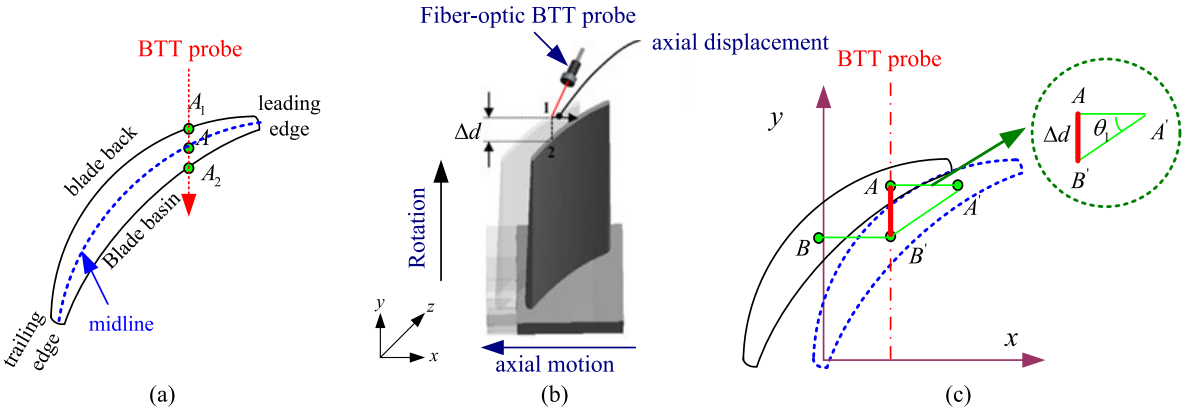

FIGURE 3. Schematic diagram under axial motion: (a) the tip profile; (b) axial displacement; (c) measurement deviation.

accuracy of blade vibration measurement. Mohamed *et al.* first discussed the change of BTT sensing positions caused by steady-state blade motions [9], [10]. But the blade was assumed to be straight. Actual engine blade always has a complex profile and the blade tip is composed of leading edge, trailing edge, blade basin and blade back, as shown in Figure 3(a). Generally speaking, the blade basin and back are two free curves, and the leading and trailing edge are two arcs. Therefore, it needs to reconsider the issue of measurement deviation. This paper will refer to the method in [9], [10] to investigate the influence mechanism of translational blade motions on vibration measurement under variable speeds. Here translational blade motions include axial motion, bending motion and radial motion.

1) AXIAL MOTION

refers to the axial motion along the axis of the rotor caused by installation error or/and aerodynamic loads, which will cause the blisk to have an overall displacement as shown in Figure 3(b). The blade tip has a certain thickness, so the laser light begins to enter the tip from the point (A_1) on the blade back and leaves the tip from the point (A_2) on the blade basin during rotation. Because the light spot has a certain radius, electric signal generated by the reflected light is not an ideal pulse. After rectification, the electric signal is converted into a square-wave signal for tip timing. Therefore, the midpoint (A) between A_1 and A_2 is looked as the BTT sensing position in this paper.

When the blisk has an overall axial displacement, the blade tip will also shift from the original position. As shown in Figure 3(c), the dotted line denotes the original tip position and the solid line denotes the new tip position after translation. It can be seen that the BTT sensing position changes from B' to A. In this case, the blade passes the BTT probe earlier than the case under no translation, which will generate the measurement deviation (Δd) of blade vibration displacement. Furthermore, Δd is defined as,

$$\Delta d = AA' \times \tan\theta_1 \tag{13}$$

where AA' denotes the translational displacement and θ_1 is the included angle.

If the blade is simplified to be straight, θ_1 is just equal to the inclination angle of the chord line relative to the rotation axis [9]. As for a blade with complex profile, however, θ_1 is not a constant but depends on the blade tip profile. In this case, Equation (13) cannot be utilized again. Furthermore, by taking the circle center of the trailing edge as the origin and the inverse translational direction as x axis, a coordinate system is built as shown in Figure 3(b). Then the curve equations of the blade back and basin can be approximated by the following polynomials, respectively.

$$\begin{aligned} y_{back}(x) &= \sum_{i=0}^{M} \eta_i x^i \\ y_{basin}(x) &= \sum_{i=0}^{N} \gamma_i x^i \end{aligned} \tag{14}$$

where the coefficients (η_i, γ_i) and the orders (M, N) can be estimated by measuring the blade tip's profile.

The x coordinate of B' is denoted as $x_{B'}$ which can be obtained in advance according to the position of the BTT probe. Then the x coordinate of A' is equal to $x_{B'} + AA'$. In this case, the y coordinates of B' and A are represented as

$$\begin{aligned} y_A &= \frac{y_{back}(x_{B'} + AA') + y_{basin}(x_{B'} + AA')}{2} \\ y_{B'} &= \frac{y_{back}(x_{B'}) + y_{basin}(x_{B'})}{2} \end{aligned} \tag{15}$$

Then the measurement deviation (Δd) is calculated as Equation (16) according to Figure 3(c).

$$\begin{aligned} \Delta d = &\frac{y_{back}(x_{B'} + AA') + y_{basin}(x_{B'} + AA')}{2} \\ &- \frac{y_{back}(x_{B'}) + y_{basin}(x_{B'})}{2} \end{aligned} \tag{16}$$

2) BENDING MOTION

refers to the first-order bending vibration of the blade due to aerodynamic loads, as shown in Figure 4(a). In this case, the

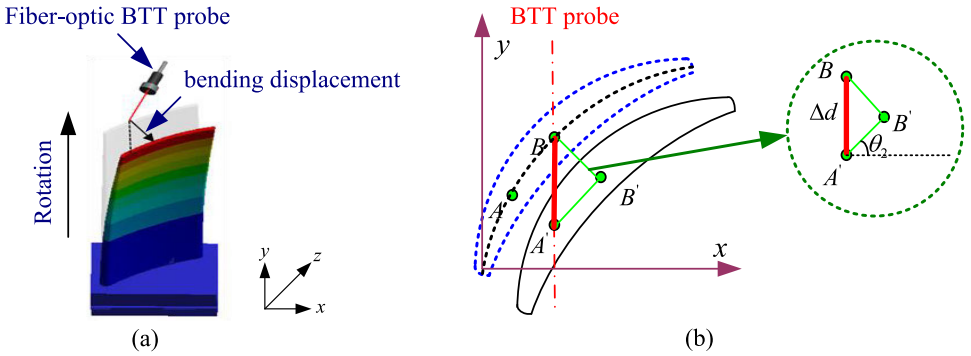

FIGURE 4. Schematic diagram under bending motion: (a) bending displacement; (b) measurement deviation.

blade tip will shift perpendicularly to the chord line of the blade. As shown in Figure 4(b), the dotted line denotes the original tip position and the solid line denotes the new tip position after bending. It can be seen that the BTT sensing position changes from B to A'. In this case, the blade passes the BTT probe later than the case under no bending, which will also generate measurement deviation (Δd). Furthermore, Δd is defined as follows according to Figure 4(b).

$$\Delta d = BB'\sqrt{1 + (\tan\theta_2)^2} \tag{17}$$

where BB' is the bending displacement and θ_2 is the included angle which is also related to the blade tip's profile.

Moreover, the curve equation of the midline of the blade tip in Figure 4(c) can be represented as

$$\begin{aligned} y_{center}(x) &= \frac{y_{back}(x) + y_{basin}(x)}{2} \\ &= \frac{\sum_{i=0}^{M} \eta_i x^i + \sum_{i=0}^{N} \gamma_i x^i}{2} \end{aligned} \tag{18}$$

Then $\tan\theta_2$ in Equation (17) can be calculated as Equation (19) by substituting Equation (18).

$$\tan\theta_2 = \left.\frac{\partial y_{center}(x)}{\partial x}\right|_{x=x_B} = \frac{\sum_{i=1}^{M-1} i\eta_i x_B^{i-1} + \sum_{i=1}^{N-1} i\gamma_i x_B^{i-1}}{2} \tag{19}$$

And the measurement deviation (Δd) is calculated as,

$$\Delta d = BB'\sqrt{4 + \left(\sum_{i=1}^{M-1} i\eta_i x_B^{i-1} + \sum_{i=1}^{N-1} i\gamma_i x_B^{i-1}\right)^2} \Big/ 2 \tag{20}$$

3) RADIAL MOTION

refers to blade translation in radial direction caused by the deformation of the rotating axis. In this case, the BTT sensing position does not change, while the tip radius will change. Therefore measurement deviation is also introduced. Radial displacement of the blade is assumed to be ΔR, then the measurement deviation (Δd) can be calculated as,

$$\Delta d = 2\pi f_n \Delta R(t_{i,k,n}^{act} - t_{i,k,n}^{the}) \tag{21}$$

IV. DERIVATION CALIBRATION OF BTT VIBRATION MEASUREMENT

A. VIBRATION CALIBRATION UNDER VARIABLE ROTATING SPEEDS

According to Equation (7), we can see that the measurement deviation under variable rotating speed mainly comes from estimation of the rotating angle in the nth revolution using the sampled TOAs. Therefore, it needs to approximate the area surrounded by $\{A_1, t_{n-1}, t_n^{\Delta}, B_3\}$ in Figure 2 in order to reduce the measurement deviation. Based on this idea, this paper presents the corresponding vibration calibration method, which is suitable for each blade passing each BTT probe. Without loss of generality, the subscripts of 'i' and 'k' will be ignored in next sections for the sake of simplicity.

1) UNDER LINEAR VARIATION

The rotating angular speed is denoted as $\omega_n(t) = \lambda t$, where λ is the unknown slope. Based on the following formula,

$$\int_{t_{n-1}}^{t_n} \omega_n(t)dt = \int_{t_{n-1}}^{t_n} \lambda t dt = 2\pi \tag{22}$$

λ can be calculated as $4\pi/\left[(t_n)^2 - (t_{n-1})^2\right]$. Then we will have

$$\begin{aligned} \omega_{n-1} &= 4\pi t_{n-1}/\left[(t_n)^2 - (t_{n-1})^2\right], \\ \omega_0 &= 4\pi t_n^{\Delta}/\left[(t_n)^2 - (t_{n-1})^2\right]. \end{aligned}$$

Furthermore, we choose $\bar{\omega} = (\omega_{n-1} + \omega_0)/2$. Then it is not hard to prove that the area surrounded by $\{A_2, t_{n-1}, t_n^{\Delta}, B_2\}$ is equal to that surrounded by $\{A_1, t_{n-1}, t_n^{\Delta}, B_3\}$ in Figure 2 (a). In this case, actual AOAs in Equation (6) can be revised as,

$$\widehat{\theta}_n^{act} = 2\pi(n-1) + 2\pi\left[\left(t_n^{\Delta}\right)^2 - (t_{n-1})^2\right]\Big/\left[(t_n)^2 - (t_{n-1})^2\right] \tag{23}$$

Obviously, the above actual AOAs are exactly accurate, so the measurement deviation can be completely calibrated under linearly varying speed.

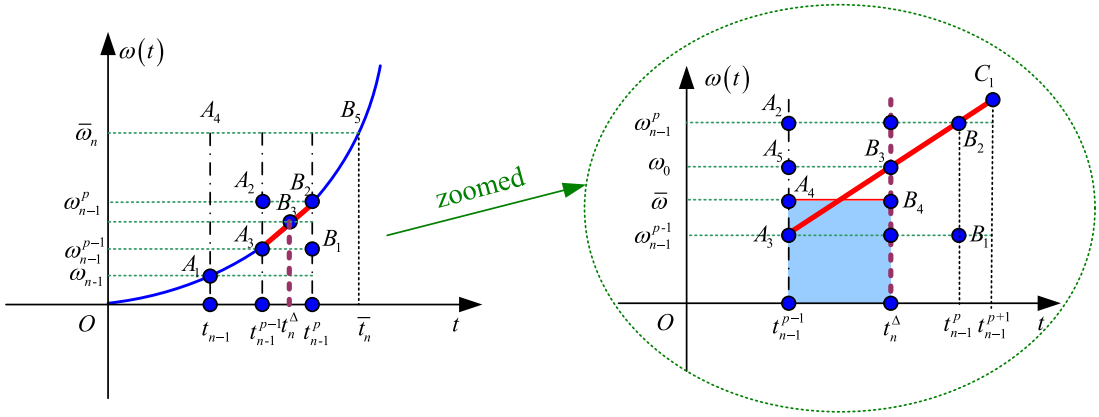

FIGURE 5. Schematic diagram of vibration calibration under quadratic variation of rotating speed.

2) UNDER QUADRATIC VARIATION

Rotating angular speed always changes fast. In this case, the area surrounded by $\{A_1, t_{n-1}, t_n^{\Delta}, B_3\}$ can be estimated by using piecewise approximation in order to reduce the derivation. For this purpose, the idea of using M uniform OPR marks on the rotating shaft can be borrowed [21]. In this case, M OPR signals will be generated during each revolution. In this paper, the M uniform OPR marks and the corresponding signals are assumed to be ideal, so that their uncertainties are ignored. As shown in Figure 5, the $(M+1)$ OPR times in the nth revolution are denoted as $\left\{t_{n-1}^0, t_{n-1}^1, \ldots, t_{n-1}^{M-1}, t_{n-1}^M\right\}$ with $t_n^{\Delta} \in \left(t_{n-1}^{p-1}, t_{n-1}^{p}\right)$, $1 \le 1 \le M$, where $t_{n-1}^0 = t_{n-1}$ and $t_{n-1}^M = t_n$. Then we will have,

$$\begin{aligned} S_{\{A_1, t_{n-1}, t_n^{\Delta}, B_3\}} &= S_{\left\{A_1, t_{n-1}, t_n^{p-1}, A_3\right\}} + S_{\left\{A_3, t_{n-1}^{p-1}, t_n^{\Delta}, B_3\right\}} \\ S_{\left\{A_1, t_{n-1}, t_n^{p-1}, A_3\right\}} &= 2\pi\,(p-1)/M \end{aligned} \tag{24}$$

where S denotes the area. Next, in order to estimate $S_{\left\{A_3, t_{n-1}^{p-1}, t_n^{\Delta}, B_3\right\}}$, three instantaneous angular speeds at t_{n-1}^{p-1}, t_{n-1}^{p}, t_{n-1}^{p+1} are assumed to be in a straight line, as shown in Figure 5. This line can be represented as,

$$\omega_n(t) = \psi_n t + b_n \tag{25}$$

where ψ_n, b_n are two unknown parameters to be identified. Furthermore, we will have,

$$\begin{cases} \int_{t_{n-1}^{p-1}}^{t_{n-1}^{p}} (\psi_n t + b_n)dt = 2\pi/M \\ \int_{t_{n-1}^{p}}^{t_{n-1}^{p+1}} (\psi_n t + b_n)dt = 2\pi/M \end{cases} \tag{26}$$

Thus ψ_n, b_n can be identified as (27a) and (27b), as shown at the bottom of the next page,

Then ω_{n-1}^{p-1} and ω_0 can be calculated as,

$$\omega_{n-1}^{p-1} = \psi_n t_{n-1}^{p-1} + b_n,\ \omega_0 = \psi_n t_n^{\Delta} + b_n \tag{28}$$

Similar to Equation (23), actual AOAs under quadratic variation of rotating speed can be approximated as,

$$\begin{aligned} \widehat{\theta}_n^{act} &= 2\pi\,(n-1) + 2\pi\,(p-1)/M + \left(\omega_{n-1}^{p-1} + \omega_0\right)\Big/2 \\ &\quad \times \left(t_n^{\Delta} - t_{n-1}^{p-1}\right) \end{aligned} \tag{29}$$

It can be understood that the measurement deviation will decrease with the increase of M. In particular, a large M should be used to reduce the deviation within the allowable range when the rotating speed changes rapidly.

B. VIBRATION CALIBRATION UNDER THE DERIVATION OF STATIC POSITION ANGLES

Based on Equation (10) and Equation (12), we can see that the measurement deviation due to static position angle (α_i or θ_k) tends to be a constant. In this case, vibration calibration can be realized by removing the mean of vibration displacements. However, such calibration method is ideally performed for just one static angle. Furthermore, it's not hard to find out that BTT vibration measurement is directly related to the relative angle between the blade and each BTT probe, i.e., $\alpha_i - \theta_k$. Therefore, this paper proposes a novel method to calibrate the relative angle (i.e., $\phi_{ik} = \alpha_i - \theta_k$), instead of a single static angle (α_i or θ_k). The most advantage is that the measurements deviation due to both α_i and θ_k can be calibrated simultaneously. The details of the method are illustrated as follows.

Angle derivation of ϕ_{ik} is denoted as $\Delta\phi_{ik}$. Firstly, the rotating speed is set to be low and slowly variable, so that the rotating period of each revolution can be considered as a constant. In the case, the period of the nth revolution is calculated as $T_n = t_n - t_{n-1}$. Theoretical TOAs of the kth blade passing the ith BTT probe can be calculated as

$$t_{i,k,n}^{the} = \begin{cases} \sum_{j=1}^{n-1} T_j + \dfrac{\phi_{ik} T_n}{2\pi},\ \theta_k \le \alpha_i \\ \sum_{j=1}^{n} T_j + \dfrac{\phi_{ik} T_n}{2\pi},\ \theta_k > \alpha_i \end{cases} \tag{30}$$

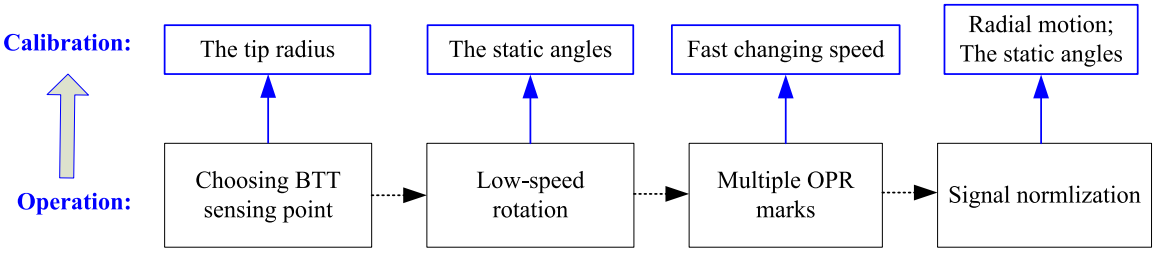

FIGURE 6. Schematic diagram of calibration process of BTT vibration measurement.

At the same time, actual TOAs can be calculated as,

$$t_{i,k,n}^{act} = \sum_{j=1}^{n-1} T_j + \Delta t_n^{ik} \tag{31}$$

Furthermore, the excitation frequency is much less than resonant frequencies of a blade under low rotating speeds, so it can be assumed that there are no blade vibrations. In theory, $t_{i,k,n}^{act}$ should be equal to $t_{i,k,n}^{the}$. In practice, however, it is not the case due to $\Delta\phi_{ik}$. The derivation calculated in the nth revolution is denoted as $\Delta\phi_{ik}^n$, which can be calculated as follows based on Equation (30) and Equation (31).

$$\Delta\phi_{ik}^n = \begin{cases} 2\pi\,\Delta t_n^{ik}/T_n - \phi_{ik}, \theta_k \le \alpha_i \\ 2\pi\left(\Delta t_n^{ik} - T_n\right)/T_n - \phi_{ik}, \theta_k > \alpha_i \end{cases} \tag{32}$$

Then $\Delta\phi_{ik}$ can be represented as the following average value during N revolutions.

$$\bar{\Delta}\phi_{ik} = \sum_{n=1}^{N} \Delta\phi_{ik}^n \Big/ N \tag{33}$$

Finally, the calibrated relative angle is written as $\tilde{\phi}_{ik} = \phi_{ik} + \bar{\Delta}\phi_{ik}$, which can be applied to calculate blade vibration displacement. By this way, the measurement deviation due to static angles can be reduced greatly.

C. VIBRATION CALIBRATION UNDER TRANSLATIONAL BLADE MOTIONS

As for axial and bending motions, it can be seen that the measurement deviation is strongly related to translational displacement of a blade. In practice, however, it is very difficult to obtain the instantaneous BTT sensing position under variable rotating speeds. Zhang *et al.* proposed to track actual measuring point position relative to the blade tip during blade rotation [21]. But it assumed that the rotating speed of each revolution was constant. Therefore, vibration calibration under axial and bending blade motions is still an open problem deserved to be further explored. While under radial motion, the BTT sensing position doesn't change and the measurement deviation just depends on ΔR. Generally speaking, ΔR is much smaller than R, so the impact is relatively small. In addition, the measurement deviation can be further reduced by signal preprocessing, such as normalization.

To sum up, in practice the calibration process of BTT vibration measurement under variable speeds can be sketched in Figure 6. Firstly, it needs to choose the optimal BTT sensing position which changes little during rotation. This task may be accomplished by finite element simulation or digital twin. That is to say, vibration displacements of the blade tip can be estimated by these two methods, so that the position with the smallest torsional motion is first chosen as the BTT sensing position. Secondly, TOAs under a preset low speed are sampled to calculate $\Delta\phi_{ik}$, so that the static angles can be calibrated. Next, if the rotating speed changes very fast, multiple OPR marks should be made to reduce measurement deviation. In the end, measured BTT vibration signals can be preprocessed by normalization to further calibrate these derivations due to radial motion or static angles.

V. SIMULATIONS AND DISCUSSIONS

A. MATLAB/SIMULINK-BASED BTT MODEL

In order to validate the proposed method, numerical simulations are done to generate BTT samples. Here a rotational blade is assumed to be a cantilever beam and only the first-order bending mode is considered. Under this assumption, dynamic behavior of the blade can be represented by a single-degree-of-freedom (SDOF) lumped-parameter model

$$\psi_n = \frac{4\pi\left(2t_{n-1}^p - t_{n-1}^{p-1} - t_{n-1}^{p+1}\right)}{M\left\{\left[\left(t_{n-1}^{p+1}\right)^2 - \left(t_{n-1}^p\right)^2\right]\left(t_{n-1}^p - t_{n-1}^{p-1}\right) - \left[\left(t_{n-1}^p\right)^2 - \left(t_{n-1}^{p-1}\right)^2\right]\left(t_{n-1}^{p+1} - t_{n-1}^p\right)\right\}} \tag{27a}$$

$$b_n = \frac{2\pi\left\{\left[\left(t_{n-1}^{p+1}\right)^2 - \left(t_{n-1}^p\right)^2\right] - \left[\left(t_{n-1}^p\right)^2 - \left(t_{n-1}^{p-1}\right)^2\right]\right\}}{M\left\{\left[\left(t_{n-1}^{p+1}\right)^2 - \left(t_{n-1}^p\right)^2\right]\left(t_{n-1}^p - t_{n-1}^{p-1}\right) - \left[\left(t_{n-1}^p\right)^2 - \left(t_{n-1}^{p-1}\right)^2\right]\left(t_{n-1}^{p+1} - t_{n-1}^p\right)\right\}} \tag{27b}$$

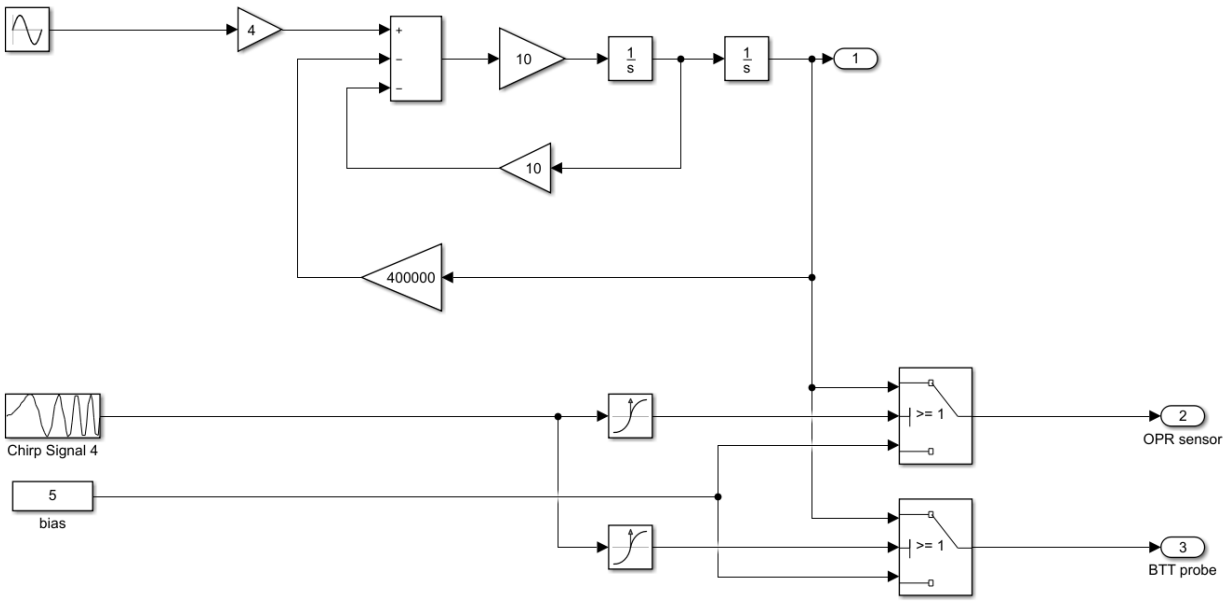

FIGURE 7. Simulink model of BTT sampling process under linear variation of rotating speeds.

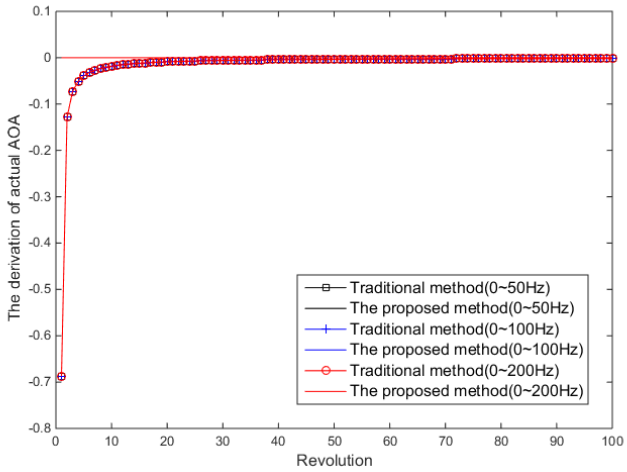

FIGURE 8. The derivation of actual AOA under Test 1.

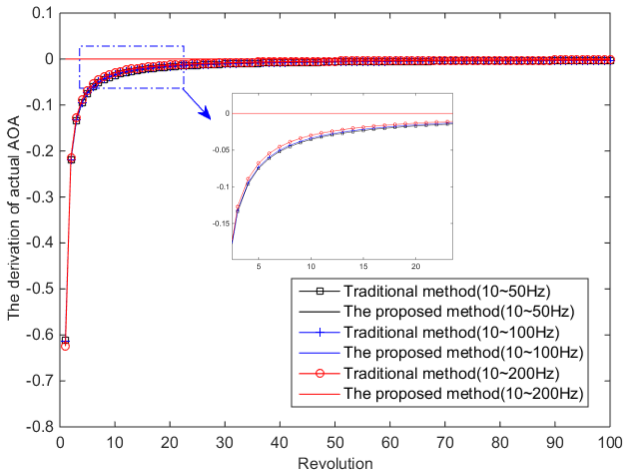

FIGURE 9. The derivation of actual AOA under Test2.

and its vibration equation is written as follows [13].

$$m_{eq}\ddot{y}(t) + c_{eq}\dot{y}(t) + k_{eq}y(t) = F(t) \tag{34}$$

where m_{eq}, c_{eq}, k_{eq} are the equivalent mass, damp and stiffness, respectively. $y(t)$ denotes blade vibration displacement. $F(t)$ denotes the vibration excitation.

Next the BTT sampling process in angular domain is simulated in Matlab/Simulink environment. Firstly, the SDOF model in Equation (34) is built. Then the sampling times of OPR and BTT probes are obtained by using the 'Hit Crossing' Block and the 'Switch' Block in the Simulink. Basic procedure is demonstrated as follows: The angle of the OPR probe relative to the OPR mark is denoted as θ_0 and the time-dependent rotating frequency is denoted as $f_r\ (t)$. For the OPR probe, the sampling time in the nth revolution can be solved by

$$2\pi \int_0^t f_r\ (t)\, t = 2\pi n + \theta_0 \tag{35}$$

For the kth rotational blade, the angular sampling time of the ith BTT probe in the nth revolution can be solved by

$$2\pi \int_0^t f_r\ (t)\, t = \theta_0 + 2\pi n + (\alpha_i - \theta_k) \tag{36}$$

In the SDOF model, parameters are chosen as $m_{eq} = 0.1$ kg, $c_{eq} = 10$ N $\cdot$ s/m, $k_{eq} = 4 \times 10^5$ N/m and the vibration excitation is selected as $F(t) = \sin(200\pi t)$.

As stated before, few existing techniques have been studied for BTT measurement uncertainties under variable rotating speeds, so the proposed angular-domain method will be compared with tradition fixed-speed method in the following simulations.

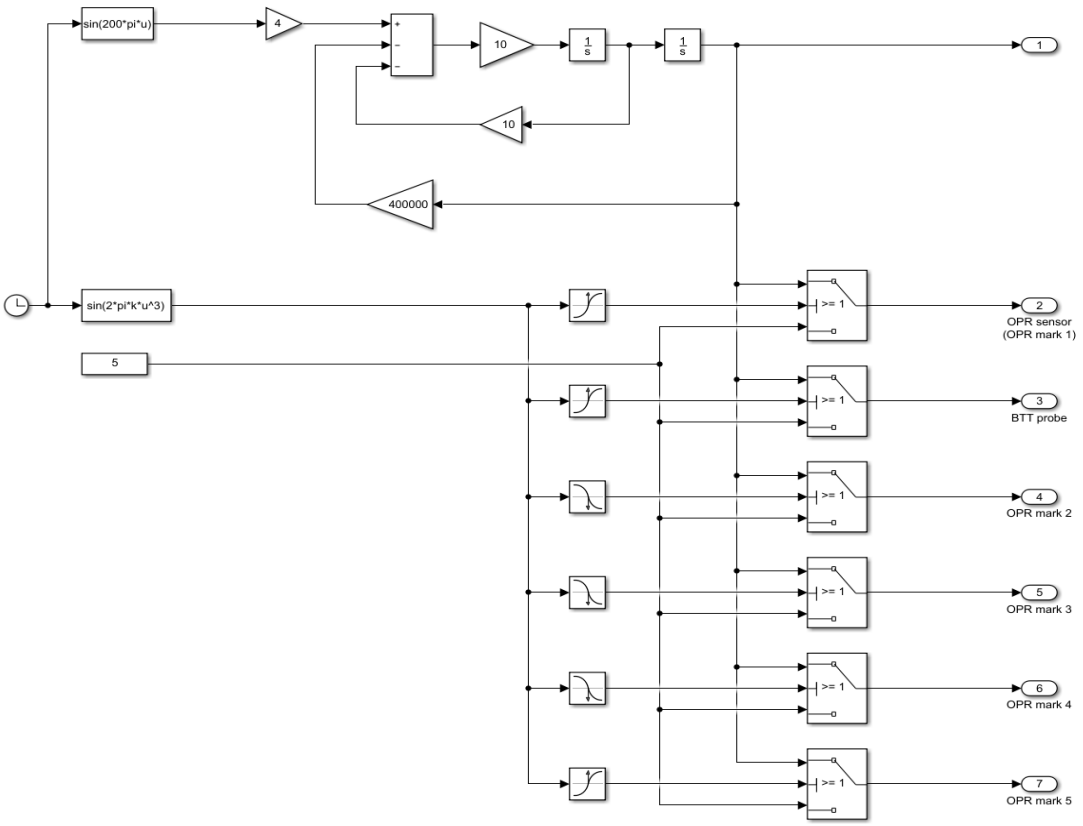

FIGURE 10. Simulink model of BTT sampling process under quadratic variation of rotating speeds.

B. CALIBRATION VALIDATION UNDER LINEARLY VARIABLE ROTATING SPEEDS

In order to simulate linearly variable rotating speeds, the rotating frequency is denoted as $f_r(t)$ which is defined as

$$f_r(t) = f_0 + (f_e - f)\, t/T_s \tag{37}$$

where f_0, f_e are the rotating frequencies at the starting time and the ending time, respectively. T_s is the total simulation time.

The Matlab/Simulink model is built as shown in Figure 7, where only an OPR mark is applied. The position angles are set as $\theta_0 = \pi/8$ and $\alpha_i - \theta_k = \pi/4$, respectively. Simulation parameters of two tests are listed in Table 1. Based on these parameters and the Simulink model in Figure 7, the OPR times and the TOAs can be obtained under each variable rotating speed. At each time step of the simulation, the output of the BTT probe is equal to sampled vibration displacement only when the blade passes the BTT probe. Otherwise, its output is equal to '5', which is not true vibration displacement. Thus the constant '5' is just used to distinguish sampled vibration displacement from other simulated outputs of the BTT probe. In this sense, the constant is not unique.

1) UNDER TEST 1

In this case, the initial rotating frequency is equal to 0. In order to simulate different degrees of linear variations, three groups of (f_e, T_s) are used as: (50, 100), (100, 50) and (200, 25). Then actual AOAs are estimated by the traditional fixed-speed method as Equation (6), and the proposed method as Equation (23), respectively. The derivation between actual and theoretical AOAs is calculated and plotted in Figure 8. We can see that: i) For each group, the derivation by the proposed method is equal to 0, much smaller than that by the traditional fixed-speed method; ii) the derivation by the traditional fixed-speed method decreases with the revolution, which means the derivation also becomes small during high-speed rotations; iii) During low-speed rotation, the derivation by the traditional fixed-speed method is obvious and non-negligible. That is to say, the traditional method cannot be used at the startup stage; iv) For different degrees of

TABLE 1. Simulation parameters under linearly variable rotating speeds.

Testing		$[f_0, f_e]$ Hz	T_s
Test 1	Case 11	[0, 50] Hz	100s
	Case 12	[0, 100] Hz	50s
	Case 13	[0, 200] Hz	25s
Test 2	Case 21	[10, 50] Hz	100s
	Case 22	[10, 100] Hz	50s
	Case 23	[10, 200] Hz	25s

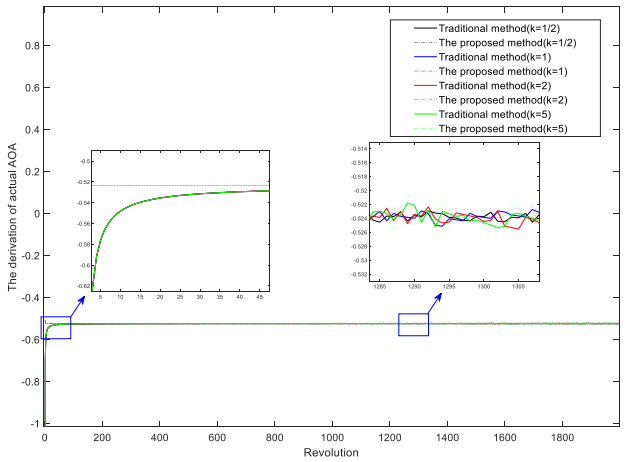

FIGURE 11. The derivation of actual AOAs under quadratic variation of rotating speeds.

linear variations, the derivations by the traditional fixed-speed method are the same, which is due to $f_0 = 0$. In order to validate it, Test 2 is carried out next.

2) UNDER TEST 2

In this case, the initial rotating frequency is equal to 10Hz. Similarly, three groups of (f_e, T_s) are used. Then actual AOAs are estimated by traditional method as Equation (6) and the proposed method as Equation (23), respectively. The derivation between actual and theoretical AOAs is calculated and plotted in Figure 9. Besides similar results in Figure 8, we can also see that: i) For different degrees of linear variations, the corresponding derivations by the traditional fixed-speed method are different during low-speed rotation when $f_0 \neq 0$, which is different from Figure 8; ii) Moreover, the faster the speed increases, the smaller the derivation is.

C. CALIBRATION VALIDATION UNDER QUADRATIC VARIATION OF ROTATING SPEED

In order to simulate quadratic variation of rotating speeds, the rotating frequency is defined as

$$f_r(t) = k_r t^2 + b_r \tag{38}$$

where k_r, b_r are two coefficients.

The Matlab/Simulink model is built as shown in Figure 10, where five ($M = 5$) OPR marks are applied. The parameters are set as $b_r = 0$ and $T_s = 20$s. Then the OPR times and the TOAs are sampled under each variable rotating speed.

Similarly, k_r is selected as 0.5, 1, 2 and 5 to simulate different quadratic variations, respectively. Then actual AOAs are estimated by the traditional fixed-speed method as Equation (6) and the proposed method as Equation (29), respectively. The derivation between actual and theoretical AOAs is calculated and plotted in Figure 11. We can see that: i) For each k_r, the derivation by the proposed method is not equal to zero, but much smaller than that by the traditional fixed-speed method at low-speed stage; For example, the derivation by the traditional method increases by 45.19% when $n = 10$;

TABLE 2. Calibration result of static angles.

Angle	Believed ϕ_{ik}	Actual ϕ_{ik}	Calibrated ϕ_{ik}
Value	45°	45.802°	45.8030°

ii) The derivation by the traditional fixed-speed method also decreases with the rotating speed.

According to Figure 8, 9 and 11, we also can see that the proposed method is much superior to the traditional fixed-speed method in the low-speed range, while the superiority is not obvious in the high-speed range. The reason is that the average speed is much close to instantaneous speed during high-speed rotation.

D. CALIBRATION VALIDATION OF STATIC ANGLES

The same Simulink model as Figure 7 is used, where the parameters are set as $f_0 = 10$Hz, $f_e = 12$Hz and $T_s = 50$s. The angle of ϕ_{ik} is set as $\pi/4$, but there is a small error $(\pi/180)$. Then actual TOAs are sampled and Equation (33) is used to estimate the angle error. The result is shown in Table 2 and we can see that ϕ_{ik} is correctly calibrated by the proposed method.

VI. CONCLUSION

Measurement uncertainties always bring serious consequence to the BTT method in practical applications. In particular, these uncertainties always become more serious under variable rotating speeds. To deal with them, this paper systematically analyzes the effects of variable rotating speed, static angle errors and translational blade motions on the accuracy of BTT vibration measurement and presents the corresponding calibration methods. The main contributions of this paper may include: i) it proposed to analyze BTT vibration measurement deviations under variable rotating speeds from the viewpoint of angular domain and the corresponding calibration process was outlined; ii) Measurement deviation due to linearly varying speed was completely calibrated by using TOAs. And measurement deviation due to nonlinearly varying speed was greatly reduced by using multiple OPR marks, such as quadratic variation of rotating speed; iii) Measurement deviation due to static angles was proved to be independent of the rotating speed and the relative angle error was calibrated under low rotating speeds. iv) Measurement deviation due to blade motions was shown to be very complex due to stochastic change of the BTT sensing point. In future work, the authors will build an experimental setup with precisely controlling blade rotating speed and carry out experimental validations. In addition, as discussed in [5], BTT measurement errors are generated by many factors, such as TOA signals, measurement noises, and so on. Thus it is worth doing deep studies on this issue. In particular, it needs to obtain accurate TOAs and more attention should be paid on translational and torsional motions of rotating blades under

variable rotating speeds in future. Also uncertainties due to multiple OPR marks also should be explored.

ACKNOWLEDGMENT

The authors would like to thank all the participants in this study.

REFERENCES

[1] A. von Flotow, M. Mercadal, and P. Tappert, "Health monitoring and prognostics of blades and disks with blade tip sensors," in *Proc. IEEE Aerosp. Conf.*, Mar. 2000, pp. 433–440.
[2] A. Ghoshal, M. J. Sundaresan, M. J. Schulz, and P. F. Pai, "Structural health monitoring techniques for wind turbine blades," *J. Wind Eng. Ind. Aerodyn.*, vol. 85, no. 3, pp. 309–324, Apr. 2000.
[3] V. Mucsi, A. S. Ayub, F. Muhammad-Sukki, M. Zulkipli, M. N. Muhtazaruddin, A. S. M. Saudi, and J. A. Ardila-Rey, "Lightning protection methods for wind turbine blades: An alternative approach," *Appl. Sci.*, vol. 10, no. 6, p. 2130, Mar. 2020.
[4] S. Heath and M. Imregun, "A survey of blade tip-timing measurement techniques for turbomachinery vibration," *J. Eng. Gas Turbines Power*, vol. 120, no. 4, pp. 784–791, Oct. 1998.
[5] Z. Chen, H. Sheng, Y. Xia, W. Wang, and J. He, "A comprehensive review on blade tip timing-based health monitoring: Status and future," *Mech. Syst. Signal Process.*, vol. 149, Feb. 2021, Art. no. 107330.
[6] S. Heath, "A new technique for identifying synchronous resonances using tip-timing," *J. Eng. Gas Turbines Power*, vol. 122, no. 2, pp. 219–225, Apr. 2000.
[7] K. Chen, W. Wang, X. Zhang, and Y. Zhang, "New step to improve the accuracy of blade tip timing method without once per revolution," *Mech. Syst. Signal Process.*, vol. 134, Dec. 2019, Art. no. 106321.
[8] W. Wang, D. Hu, Q. Li, and X. Zhang, "An improved non-contact dynamic stress measurement method for turbomachinery rotating blades based on fundamental mistuning model," *Mech. Syst. Signal Process.*, vol. 144, Oct. 2020, Art. no. 106851.
[9] M. Mohamed and B. Philip, "The determination of steady-state movements using blade tip timing data," in *Proc. ASME Turbo Expo. Turbomachinery Tech. Conf. Expo.*, Oslo, Norway, Jun. 2018, Art. no. V07CT35A010.
[10] M. E. Mohamed, P. Bonello, and P. Russhard, "Determination of simultaneous steady-state movements using blade tip timing data," *J. Vibrat. Acoust.*, vol. 142, no. 1, Feb. 2020, Art. no. 011017.
[11] P. Russhard, "Blade tip timing (BTT) uncertainties," in *Proc. AIP Conf.*, vol. 1740, no. 1, 2016, Art. no. 020003.
[12] O. Jousselin, P. Russhard, and P. Bonello, "A method for establishing the uncertainty levels for aero-engine blade tip amplitudes extracted from blade tip timing data," in *Proc. 10th Int. Conf. Vibrations Rotating Machinery*, 2012, pp. 211–220.
[13] C. Zhou, H. Hu, F. Guan, and Y. Yang, "Modelling and simulation of blade tip timing uncertainty from rotational speed fluctuation," in *Proc. Prognostics Syst. Health Manage. Conf. (PHM-Harbin)*, Jul. 2017, pp. 1–5.
[14] T. M. Pickering, "Methods for validation of a turbomachinery rotor blade tip timing system," M.S. thesis, Dept. Mech. Eng., Virginia Polytech. Inst. State Univ., Blacksburg, VA, USA, 2014.
[15] M. Mohamed, P. Bonello, and P. Russhard, "Uncertainties in the calibration process of blade tip timing data against finite element model predictions," in *Proc. 12th Int. Conf. Vibrations Rotating Machinery Conf.*, Oct. 2020, pp. 298–311.
[16] Z. Chen, J. Liu, C. Zhan, J. He, and W. Wang, "Reconstructed order analysis-based vibration monitoring under variable rotation speed by using multiple blade tip-timing sensors," *Sensors*, vol. 18, no. 10, p. 3235, Sep. 2018.
[17] H. Sheng, Z. Chen, Y. Xia, and W. Wang, "Compressed sensing-based blade tip-timing vibration reconstruction under variable speeds," in *Proc. Int. Conf. Sens., Meas. Data Anal. Era Artif. Intell. (ICSMD)*, Oct. 2020, pp. 485–490.
[18] Z. Chen, H. Sheng, and Y. Xia, "Multi-coset angular sampling-based compressed sensing of blade tip-timing vibration signals under variable speeds," *Chin. J. Aeronaut.*, vol. 34, no. 9, pp. 83–93, Sep. 2021.
[19] C. W. Fan, Y. D. Wu, P. Russhard, and A. Wang, "An improved blade tip-timing method for vibration measurement of rotating blades during transient operating conditions," *J. Vib. Eng. Technol.*, vol. 8, pp. 859–868, Dec. 2020.
[20] Z. Ji-Wang, Z. Lai-Bin, D. Ke-Qin, and D. Li-Xiang, "Blade tip-timing technology with multiple reference phases for online monitoring of high-speed blades under variable-speed operation," *Meas. Sci. Rev.*, vol. 18, no. 6, pp. 243–250, Oct. 2018.
[21] X. Zhang, W. Wang, K. Chen, W. Li, D. Zhang, and L. Tian, "Five dimensional movement measurement method for rotating blade based on blade tip timing measuring point position tracking," *Mech. Syst. Signal Process.*, vol. 161, Dec. 2021, Art. no. 107898.

ZHONGSHENG CHEN (Member, IEEE) was born in Anhui, China, in 1977. He received the B.S., M.S., and Ph.D. degrees in mechanical engineering from the National University Defense Technology, Changsha, China, in 1999, 2001, and 2004, respectively.

From 2004 to 2017, he worked as a Lecture and an Associate Professor with the College of Mechatronic Engineering and Automation, National University of Defense Technology. Since July, 2017, he has been worked as a Professor with the College of Electrical and Information Engineering, Hunan University of Technology. His current research interests include nonlinear vibration energy harvesting, embedded fault diagnosis and prognostics, and condition monitoring.

YEMEI XIA was born in Hunan, China, in 1996. She received the B.S. degree in electrical engineering from the Hubei Institute for Nationalities, Enshi City, in 2019. She is currently pursuing the master's degree in electrical engineering with the Hunan University of Technology, China.

Her research interest includes BTT vibration monitoring.

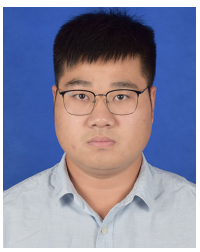

HAO SHENG was born in Anhui, China, in 1994. He received the B.S. degree in electrical engineering from Fuyang Normal College, Anhui, in 2018. He is currently pursuing the master's degree in electrical engineering with the Hunan University of Technology, China.

His research interest includes BTT vibration monitoring.

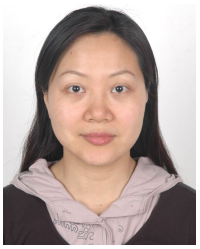

JING HE was born in Zhuzhou, China, in 1971. She received the B.S. degree in computer engineering from the National University Defense Technology, Changsha, China, in 1998, the M.S. degree in computer engineering from the Central South University of Forestry and Technology, Changsha, in 2002, and the Ph.D. degree in mechanical engineering from the National University Defense Technology, in 2009.

From 1998 to 2004, she was a Lecturer with the College of Electrical and Information Engineering, Hunan University of Technology, where she was an Associate Professor with the College of Electrical and Information Engineering, from 2004 to 2009. Since 2009, she has been a Professor with the College of Electrical and Information Engineering, Hunan University of Technology. Her research interests include nonlinear control, condition monitoring, and vibration energy harvesting.